Neurochemistry International 124 (2019) 141–151

Contents lists available at ScienceDirect

Neurochemistry International

journal homepage: www.elsevier.com/locate/neuint

Valproic acid attenuates global cerebral ischemia/reperfusion injury in gerbils via anti-pyroptosis pathways

Shu Zhu[a], Zhe Zhang[b], Lian-qun Jia[c], Kai-xuan Zhan[c], Li-jun Wang[d], Nan Song[c], Yue Liu[b], Yan-yan Cheng[b], Yong-ju Yang[b], Le Guan[b], Dong-yu Min[b,*,1], Guan-lin Yang[c,**,1]

[a] Department of Pediatric Dentistry, School of Stomatology, China Medical University, Shenyang, 110002, China
[b] The Affiliated Hospital of Liaoning University of Traditional Chinese Medicine, Shenyang, 110032, China
[c] Key Laboratory of Minstry of Education for TCM Viscera State Theory and Applications, Liaoning University of Traditional Chinese Medicine, Shenyang, 110847, China
[d] Department of Pharmacy, Beijing Ditan Hospital, Capital Medical University, Beijing, 100015, China

ARTICLE INFO

Keywords:
VPA
Ischemic/reperfusion
Pyroptosis
ARC

ABSTRACT

Ischemic stroke is the third most common cause of death and the leading cause of disability worldwide in adults. The antiepileptic drug valproic acid (VPA) was reported to protect cerebral ischemia/reperfusion injury. However, the action mechanism of VPA in cerebral ischemia/reperfusion injury has not been fully understood. We explored the action mechanism of VPA in vivo and in vitro. Gerbils were subjected to transient global cerebral ischemic–reperfusion injury, and hippocampal neuron injury was treated with oxygen-glucose deprivation in vitro. Morris water maze test was performed to evaluate the cognitive dysfunction. Histopathological examinations and western blot were performed to evaluate the pyroptosis of neurons. The results showed that VPA attenuated the cognitive dysfunction, pyroptosis of the gerbils suffer from ischemic–reperfusion injury and decreased hippocampal neurons pyroptosis induced by oxygen-glucose deprivation in vitro. In addition, western blot and real-time PCR analysis revealed that VPA modulated the protein expression of apoptosis repressor with caspase recruitment domain (ARC), caspase-1 and IL-1β/IL-18. Our results suggested that VPA alleviated ischemic/reperfusion injury-mediated neuronal impairment by anti-pyroptotic effects.

1. Introduction

Stroke, also known as cerebrovascular accident (CVA), is one of the leading causes of mortality and morbidity worldwide. There are two kinds of stroke including ischemic and hemorrhagic stroke (Donnan et al., 2008). It happens when blood flow to your brain stops. Within minutes, brain cells begin to die. It is more likely to leave sequelae and requires long-term rehabilitation and care that increase family burden and medical expenses. However, clinical data have demonstrated remarkably worse short- and long-term outcomes and higher mortality in patients after stroke because of the short therapeutic time window for recanalization therapies (Goldstein and Rothwell, 2008). Therefore, another strategy for expanding the therapeutic time window of stroke therapy is needed.

Valproic acid (VPA), a simple eight-carbon branched-chain fatty acid, has a long history of use in epileptic seizures and bipolar disorder (Gurvich and Klein, 2002). In recent years, its multiple physiological actions were well-studied in different fields, such as anticancer (Blaheta et al., 2005), neurotrophic effects (Kim et al., 2007), and anti-inflammatory, anti-immunity (Zhang et al., 2012). Inhibitory effects of VPA on fast Na and high-voltage-activated calcium currents, and lipopolysaccharide-induced production of TNF-α and IL-6 was reported (Peng et al., 2005). In addition, VPA has been reported to be a very potent inhibitor of IL-1β, IL-4, IL-6 and IL-17 production (Fantuzzi and Dinarello, 1999). However, less is known about the detailed mechanism of the effects of VPA on cerebral ischemia/reperfusion injury.

Pyroptosis, unlike apoptosis or necrosis, is a novel form of programmed cell death (Coll et al., 2011; Kroemer et al., 2009). The initiation of pyroptosis depend on caspase enzymes −1 (caspase-1), and accompanied by the release of a large number of pro-inflammatory

* Corresponding author. The Experimental Center of Traditional Chinese Medicine, The Affiliated Hospital of Liaoning University of Traditional Chinese Medicine, Shenyang, 110032, China.
** Corresponding author. Key Laboratory of Ministry of Education for Traditional Chinese Medicine Viscera-State Theory and Applications, Liaoning University of Traditional Chinese Medicine, 79 Chongshan Eastern Road, Huanggu, Shenyang, Liaoning, 110847, China.
E-mail addresses: Lianxin_zs@163.com (S. Zhu), mindongyu@163.com (D.-y. Min), guanli19621010@163.com (G.-l. Yang).
[1] These authors contributed equally to this work.

https://doi.org/10.1016/j.neuint.2019.01.003
Received 12 April 2018; Received in revised form 11 December 2018; Accepted 2 January 2019
Available online 03 January 2019
0197-0186/

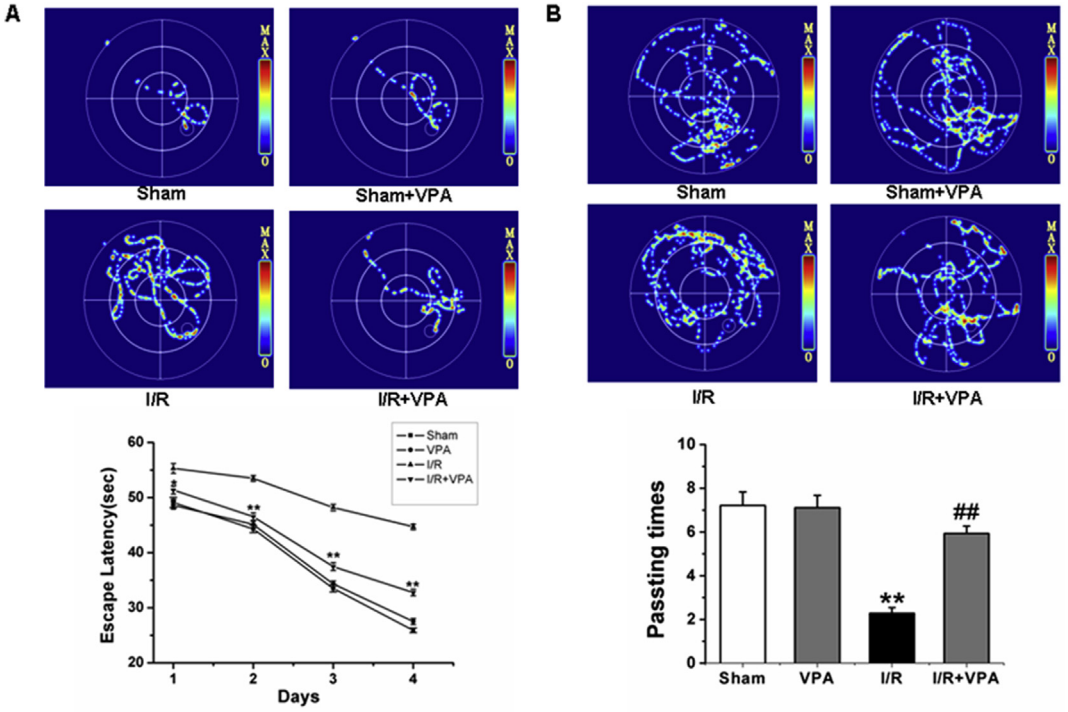

Fig. 1. VPA ameliorated ischemia/reperfusion -induced cognitive impairment in gerbils. Escape latency (A), and passing times (B) are shown in the Sham, Sham + VPA, I/R and I/R + VPA. The data are expressed as the mean ± SEM (n = 10 per group). **P < 0.01 compared to sham group; $^{\#\#}$P < 0.01 compared to I/R group.

factors (Xu et al., 2014). Caspase-1 is activated during pyroptosis by a large supramolecular complex termed the pyroptosome and processes the proforms of the inflammatory cytokines, IL-1β and IL-18, to their active forms (Byrne et al., 2013). However, few studies have focused on the participation of VPA in pyroptosis in cerebral ischemia/reperfusion injury.

The aim of this study was to elucidate whether VPA has neuroprotective effects on cerebral ischemia/reperfusion injury and, if so, to examine whether the mechanisms of neuroprotection are associated with inhibition of pyroptosis.

2. Materials and methods

2.1. Animals and treatment

Adult male Mongolian gerbils weighing between 60 and 80 g were used in the present study. All experimental protocols were pre-approved by the Experimental Animal Ethic Committee of Liaoning University of Traditional Chinese Medicine, China (Animal Experimental Ethical Inspection Protocol No. 21000092017069). Use of animals was confirmed with the Guide for the Care and Use of Laboratory Animals published by the US National Institutes of Health (NIH Publication No. 85-23, revised 1996).

2.2. Animals and induction of global brain ischemia

Transient global ischemia/reperfusion (I/R) was induced according to the method described previously with minor modification (Li et al., 2014; Zhang et al., 2009). For short, gerbils were anesthetized with an intraperitoneal injection of chloral hydrate (300 mg/kg). The bilateral common carotid arteries were exposed through a 2 cm ventral midline cervical incision and separated carefully from the vagus nerves, then occluded bilaterally for 5 min using non-traumatic aneurysm clips. Five minutes later, the clips were removed to restore cerebral blood flow. Complete reperfusion of the arteries was verified by direct visualization and the neck incision area was then sutured. The gerbils were kept under a heating pad and lamp for 2 h until recovery to prevent hypothermia. The gerbils were randomly divided into four groups: (1) Control; (2) Control + VPA group: The normal gerbils were treated with VPA intraperitoneally for1week (3) I/R group; (4) I/R + VPA group: transient global ischemia/reperfusion gerbils were subjected to VPA intraperitoneally for 1 week. The control group only received an injection of same amount of saline.

2.3. Morris water maze test

The Morris water maze tests were conducted to assess the learning and memory performance from the 7th day. Briefly, on days 1, gerbils were trained to find the platform. On days 2–5, each gerbil was subjected to three trials per day and the latency to climb onto the hidden platform was recorded in a maximum of 60 s. On the 6th day, the hidden platform was removed and the number of passing times the gerbils crossed the place where the hidden platform was previously located was recorded.

2.4. Nissl staining

The gerbils brains were removed at the 7th day, fixed in 4% paraformaldehyde for 48 h and then cryoprotected by infiltration with 30% sucrose for 3 days at 4 °C. Coronal sections (7 μm) of the hippocampus were cut and submerged in 0.1% cresyl violet for 10 min at 37 °C and then were rinsed in distilled water and dehydrated in graded ethanol covers lipped with neutral balsam. For Nissl staining, the normal neurons were round, and the nuclei appeared as pallid blue. In the ischemia/reperfusion group, the cells were shrunken, and the nuclei displayed pyknosis. Quantitative assessment of the number of live neurons in CA1 region with 10 randomly chosen high-power fields.

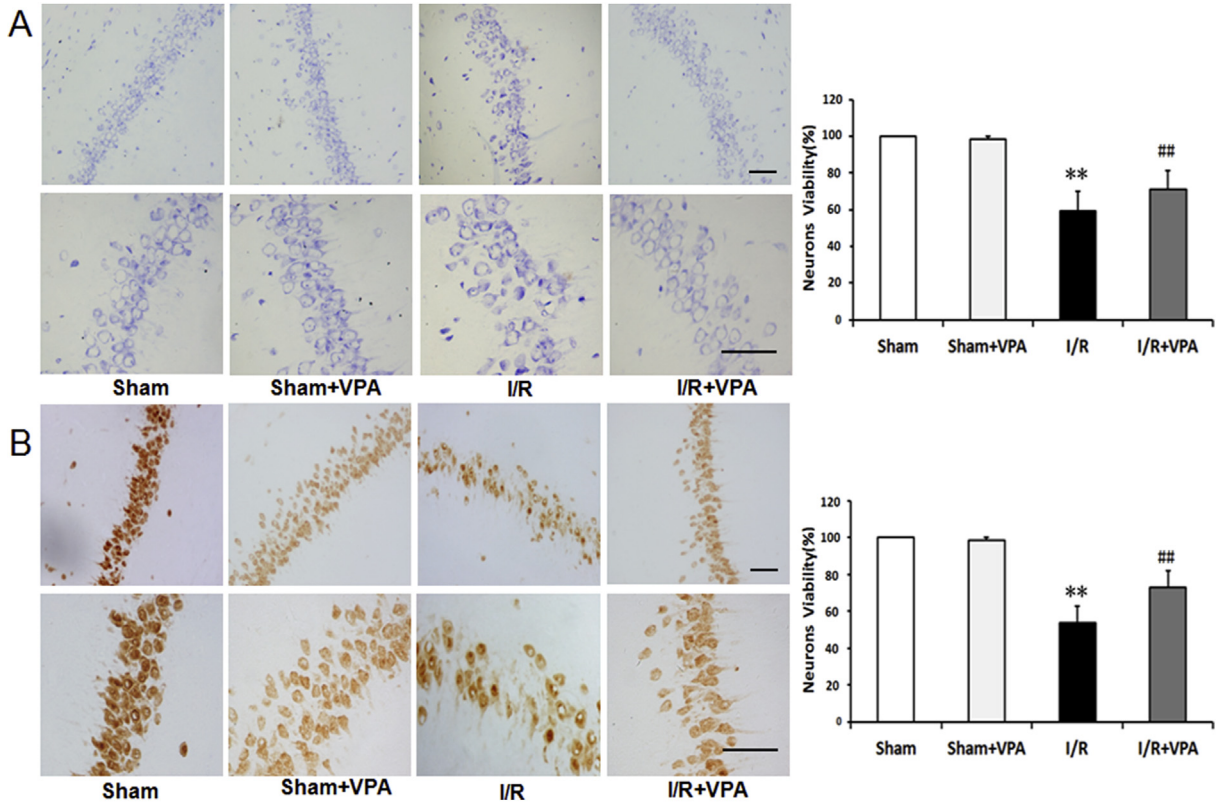

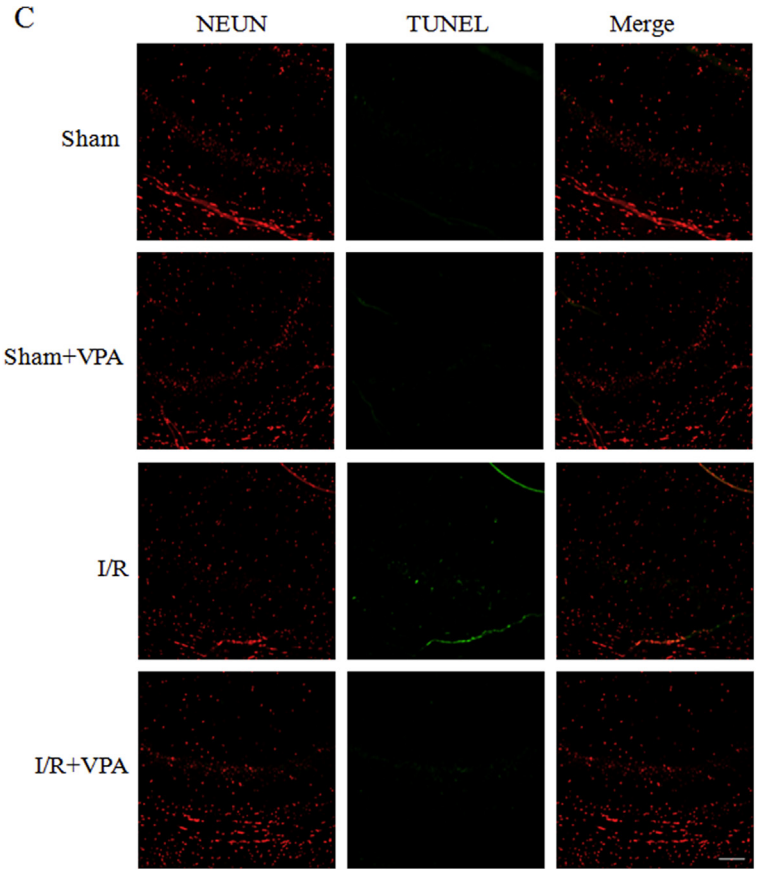

(caption on next page)

Fig. 2. Nissl staining and NeuN immunohistochemistry showed the protective effects of VPA on ischemia/reperfusion induced neuronal impairment of the hippocampal CA1 region in gerbils. (A) Representative photomicrographs of Nissl staining for surviving neurons in hippocampal CA1 region. (B) Representative immunohistochemical photomicrographs of NeuN in gerbils hippocampus. (C) Representative TUNEL/NeuN double staining in gerbils hippocampus. NeuN-positive cell (Red), TUNEL-positive cell (Green). There were fewer NeuN and Nissl-positive neurons and more TUNEL-positive neurons in the ischemia/reperfusion group than in the sham group. With treatment with VPA, NeuN and Nissl-positive neurons were abundant and TUNEL-positive neuronsin were decreased in the CA1 region compared with I/R group. Up panel is lower magnification image (200 ×) and down panel is higher magnification image (400 ×) of CA1 pyramidal neurons. Scale bar: 50 μm.

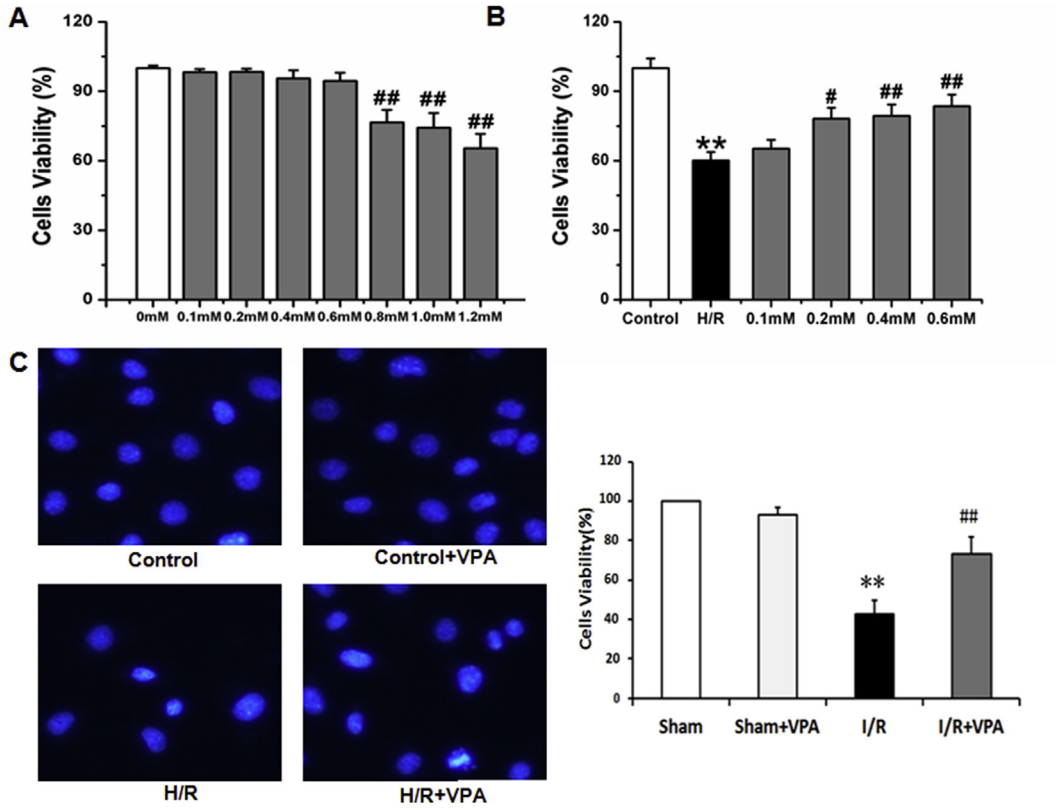

Fig. 3. VPA protects cultured hippocampal neurons from H/R injure-induced cell death. To select drug concentrations for the subsequent experiments, MTT assay was carried out on the hippocampal neurons. (A) Hippocampal neurons were treated with 0–1.2 mM VPA. (B) Hippocampal neurons were treated with H/R and then exposed to different doses of carvacrol. On the basis of the above results, hippocampal neurons treated with 0.6 mM VPA after H/R were selected. (C) Cells were observed by fluorescence microscopy after the nuclei were stained with the fluorescent dye Hoechst 33342. All the values are presented as mean ± SEM (n = 6 per group). **P < 0.01 compared to control group; ##P < 0.01 compared to H/R group. Scale bar: 50 μm.

2.5. NeuN immunohistochemistry

Hippocampus injury was evaluated based on the results of Nissl staining and immunohistochemistry in brain sections. Tissue sections were treated with 0.3% hydrogen peroxide (H_2O_2) for 10 min and then non-specific antibody binding was blocked with 10% goat serum for 30 min at room temperature. The sections were incubated with mouse anti-NeuN (1:200, Chemicon, CA) overnight at 4 °C, and subsequently, the sections were exposed to biotinylated goat anti-mouse IgG and streptavidin peroxidase complex (Vector, Burlingame, CA) for 30 min at 37 °C. They were soaked in 3,3-diaminobenzidine (DAB), and the reaction was stopped with distilled water. The stained sections were observed under a light microscope. Quantification of the number of NeuN-immunopositive cells in CA1 region with 10 randomly chosen high-power fields.

2.6. Hippocampal neurons culture

Primary hippocampal neurons were prepared as described previously with minor modification (Almeida et al., 2005). Briefly; the hippocampus was dissected and chopped into 1 mm^3 pieces under a light microscope. The hippocampal chunks were digested in calciumand magnesium-free Hanks' balanced salt solution (HBSS) containing 0.125% trypsin in a humidified 95% air, 5% CO_2 incubator for 10 min and then resuspended in DMEM supplemented 10% fetal bovine serum (FBS) in order to stop trypsin activity. After centrifugation at 140*g* for 5 min, the cell pellet was resuspended and mechanically dissociated in HBSS. Hippocampal cultures were maintained in serum-free Neurobasal medium, supplemented with B27 supplement in a humidified atmosphere (95% air, 5% CO_2) at 37 °C for 7–8 d, the time required for maturation of hippocampal neurons.

2.7. Hippocampal neurons hypoxia/reoxygenate model

Hypoxia/reoxygenate (H/R) of gerbils hippocampal neurons were carried out as described previously (Wu et al., 2003) with some modification. Briefly, after the indicated times, culture plates were transferred into a modular hypoxia chamber (Modular Incubator Chamber MIC-101; Billups-Rothenberg, Inc., Del Mar, CA, USA) in 94% N_2, 5% CO_2, and 1% O_2 atmosphere, and incubated at 37 °C for 4 h. To reoxygenate hypoxic cells, culture plates were placed in a normoxic incubator (95% air, 5% CO_2) and incubated at 24 h for further experiments.

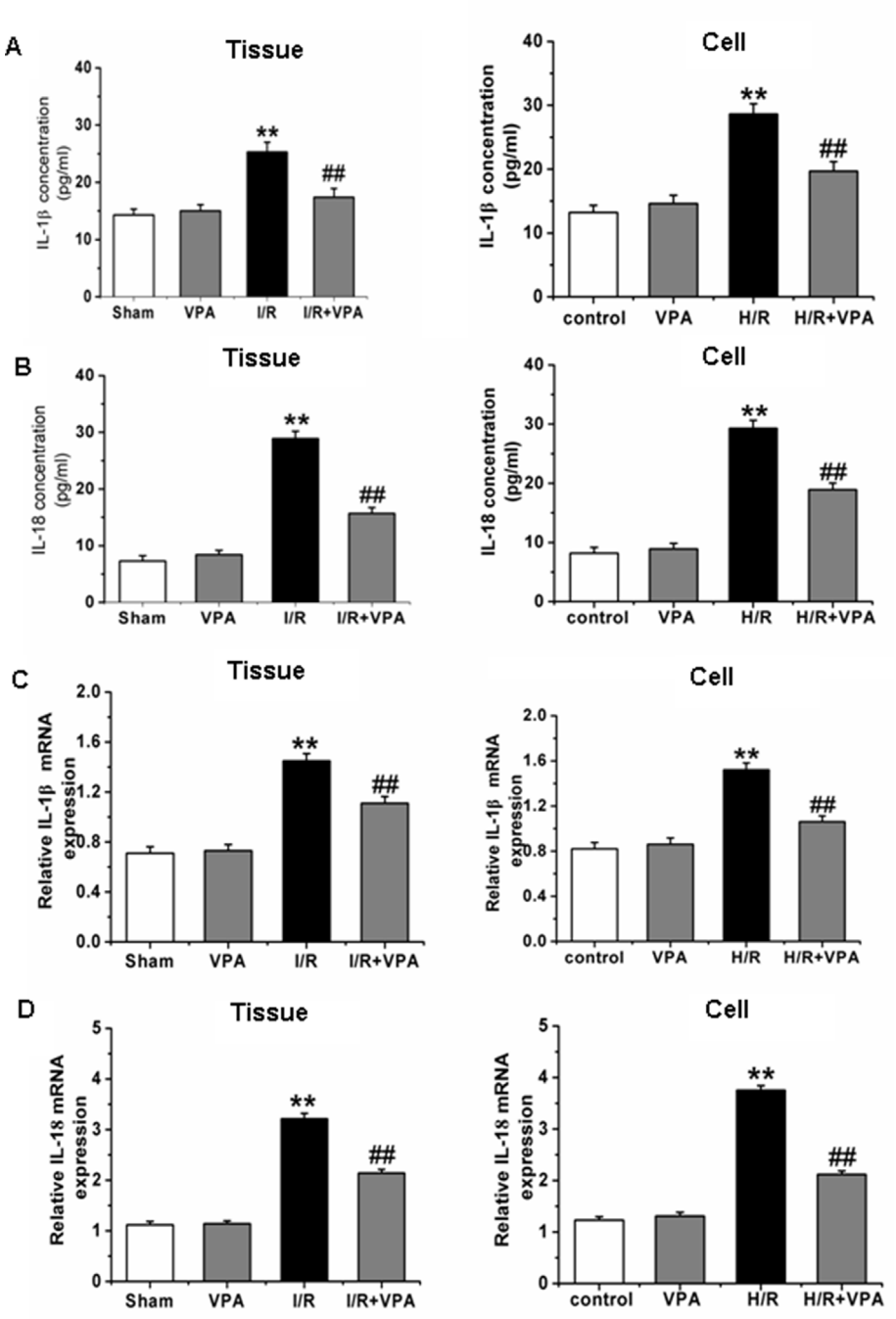

Fig. 4. VPA inhibited hippocampal neurons pyroptosis in vivo and in vitro. IL-1β (A) and IL-18 (B) concentrations in the gerbils hippocampal tissue and hippocampal neurons, respectively. IL-1β (C), IL-18 (D) mRNA expression in the gerbils hippocampal tissue and hippocampal neurons, respectively. IL-1β (E) and IL-18 (F) protein expression in the gerbils hippocampal tissue and hippocampal neurons, respectively. All the values are presented as mean ± SEM (n = 6 per group). **P < 0.01 compared to control group; ##P < 0.01 compared to H/R or I/R group.

2.8. Hoechst staining

Hippocampal neurons were grown on in six-well plates. After drug treatments, cells were fixed with 4% paraformaldehyde for 4 °C overnight. Fixed cells were then washed with PBS three times and stained with Hoechst 33258 (final concentration, 0.5 μg/ml) for 5 min. The six-well plates were visualized using a fluorescent microscope (IX51, Olympus).

2.9. Hippocampal neurons viability assay

Hippocampal neurons were plated at 35,000 cells/well in a 96-well plate. Cell viability was assessed after VPA treatments. According to the manufacturer's recommendations, 40 μl MTT solution was added into each of the wells, and absorbance were obtained at 490 nm using a microplate reader (FlexStation 3; MolecularDevices, Sunnyvale, CA, USA). The same volume of medium without cells was used as blank.

2.10. Western blot

Samples with an equal amount of protein (50 μg) were separated in SDS- polyacryl-amide gels and then transferred onto nitrocellulose membranes (Millipore, MA). The membranes were then blocked using 5% fat-free milk for 1 h and then were incubated with the following

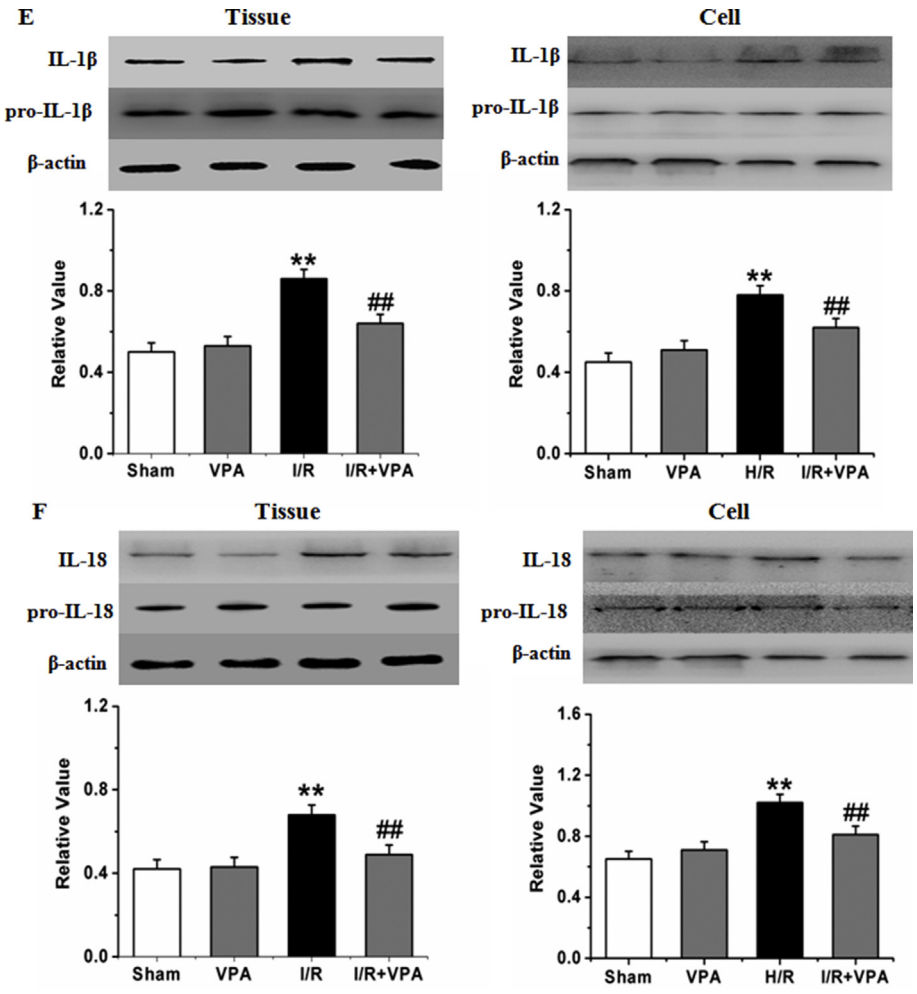

Fig. 4. (*continued*)

primary antibodies: rabbit anti-caspase-1 (1:300, Santa Cruz), rabbit anti-ARC (1:200, Santa Cruz), rabbit anti-NLRP1/3 (1:500, Novus Biologicals), rabbit anti-IL-18 (1:500, abcam), rabbit anti-IL-1β (1:500, abcam) respectively, overnight at 4 °C. The membranes were washed with TBS-T, followed by the incubation with horseradish peroxidase-conjugated goat antirabbit antibody (1:5000, Santa Cruz), for 2 h at room temperature. Immunoreactive bands were visualized by enhanced chemiluminescence (ECL) kit (Pierce, CA) and exposed on an X-ray film. The immunoblots intensities were quantified using the Quantity One software (BioRad).

2.11. Real-time PCR

Equal amounts of RNA (500 ng) from each sample was reverse transcribed in a volume of 10 μl to produce cDNA using Takara RNA PCR Kit (AMV) Ver 3.0 (TaKaRa Bio Inc.). SYBR Green I-based detection was conducted on a real-time PCR instrument (ABI PRISM 7300) with thermal cycler conditions as follows: 95 °C for 30 s, followed by 45 cycles (95 °C for 10 s and 62 °C for 31 s). All experiments were repeated twice, and in each experiment, samples were assayed in duplicate.

The following primers were used in the study:

ARC:
Forward, 5′-ATGGGTAACATGCAGGAGCGC-3′,
Reverse, 5′-GTCCAGCAGCAACCCAGAGTC-3′;
Caspase-1:
Forward, 5′-ACACGTCTTGCCCTCATTATCT-3′,
Reverse, 5′-ATAACCTTGGGCTTGTCTTTCA-3′;
IL-1β:
Forward, 5′-CCCTGCAGCTGGAGAGTGTGG-3′,
Reverse, 5′-TGTGCTCTGCTTGAGAGGTGCT-3′;
IL-18:
Forward, 5′-ACAACCGCAGTAATACGGAGCA-3′,
Reverse, 5′-TGTGCTCTGCTTGAGAGGTGCT-3′.

2.12. ELISA

Double-antibody sandwich enzyme-linked immunosorbent assay (ELISA) was employed to detect the levels of pro-IL-1β, IL-18 and mature IL-1β, IL-18 in the in the hippocampal neurons and gerbils hippocampal tissue, respectively. Detection was performed according to the manufacturer's instructions.

Transfection procedures for transfection, cells were washed with serum free medium once and then incubated with 4 ml serum-free medium for 4–6 h. The siRNA (ARC) and lipofectamine 2000 (Invitrogen) were separately mixed with 500 μl of Opti-MEM I Reduced Serum Medium (Gibco, Grand Island, NY) for 5 min. Then, the two mixtures were combined and incubated at room temperature for 18 min. The lipofectamine: siRNA (ARC) mixture was added to the cells and incubated at 37 °C for 6 h. Subsequently, 5 ml of fresh medium containing 10% fetal bovine serum was added to the flasks, and the cells were maintained in culture until the following experiments.

2.13. Immunofluorescence staining

For in situ apoptosis detection, the ApopTag Kit (Oncor, Gaithersburg, MD) was used according to the manufacturer's

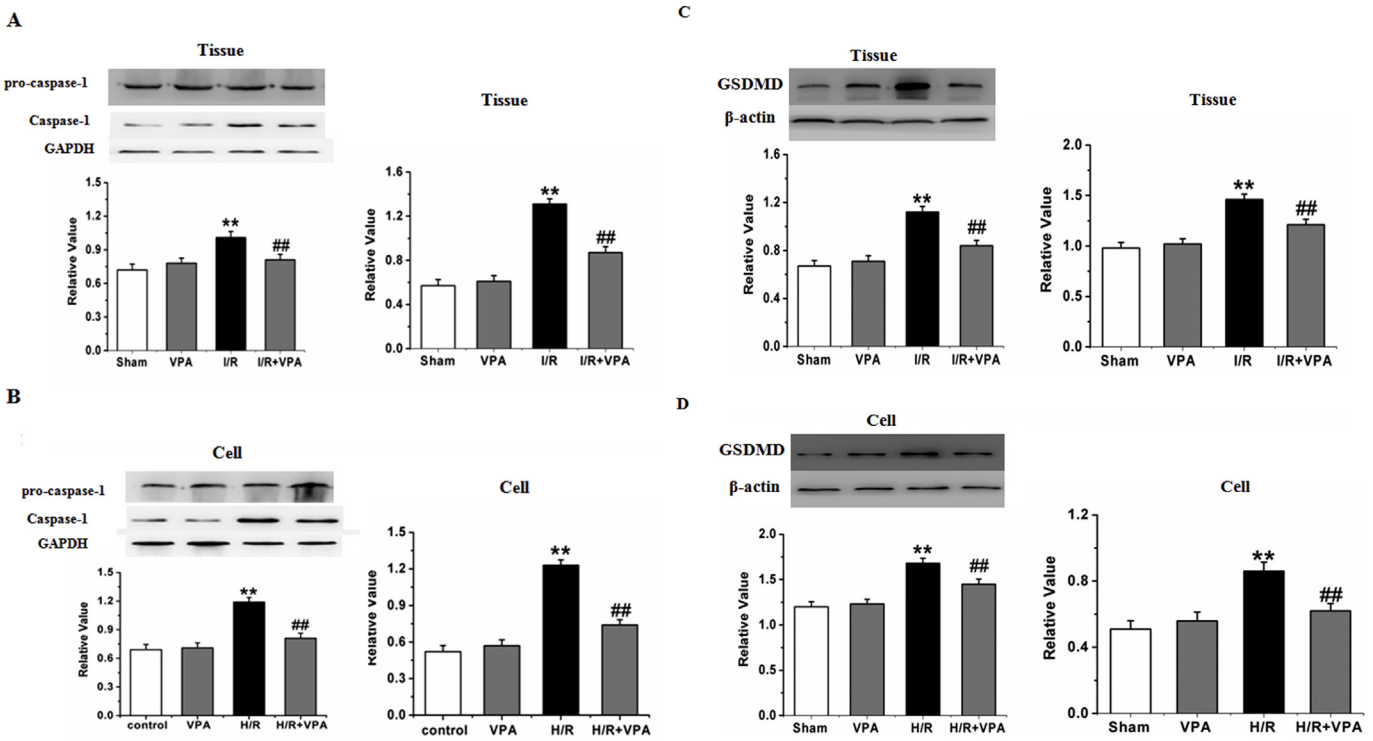

Fig. 5. VPA regulates the activity of caspase-1 in vivo and in vitro. Caspase-1 protein and mRNA expression was detected in the gerbils hippocampal tissue (A) and hippocampal neurons (B). GSDMD protein and mRNA expression was detected in the gerbils hippocampal tissue (C) and hippocampal neurons (D). NLRP1 (E,F) and NLRP3 (G,H) protein and mRNA expression was detected in the gerbils hippocampal tissue and hippocampal neurons. All the values are presented as mean ± SEM (n = 6 per group). **P < 0.01 compared to control group; $^{\#\#}$P < 0.01 compared to H/R or I/R group.

instructions. The method used is based on the biochemical property of terminal deoxynucleotidyl transferase (TdT), which catalyzes a template-independent addition of deoxyribonucleotide triphosphate to the 39-OH ends of double- or single-stranded DNA. After completing the protocol, slides were photographed at high magnification (×400) on a color slide film using a fluorescent microscope with a 590-nm filter (for fluorescence staining).

2.14. Statistics analysis

All data were analyzed using SPSS 15.0 software, and the results are expressed as the mean ± SEM. Statistical comparisons were performed with one-way analysis of variance (ANOVA) followed by Post Hoc Tukey tests. The differences in latency times in the Morris water maze were analyzed using a two-way ANOVA. P < 0.05 was considered to be statistically significant.

3. Results

3.1. VPA relieve cognitive deficits in gerbils after global cerebral ischemia/reperfusion (I/R)

As we know, ischemic stroke occurs when arteries are blocked by blood clots, and comply with neuropsychological sequelae such as depression and cognitive impairment. In order to evaluate VPA alleviating cognitive deficits in gerbils after global cerebral I/R, Morris water maze test was used. The escape latency of I/R group significantly increased in comparison to sham group (P < 0.01), while VPA treated in I/R animals reversed this effect (P < 0.01). There was no significant difference between Control and Control + VPA group (P > 0.05) (Fig. 1A). This result was confirmed by mean passing times (Fig. 1B). As a whole, VPA partially relieve cognitive impairment in gerbils after global cerebral ischemia/reperfusion.

3.2. VPA protected neuronal loss in gerbils after global cerebral ischemia/reperfusion

To explore the effects of VPA on neuronal loss induced by global cerebral ischemia/reperfusion injury, Nissl staining was examined. As show in Fig. 2A, gerbils in Control and Control + VPA group did not show any histopathological abnormalities; however, massive damaged neurons with pycnotic nucleus were observed in ischemic gerbils. VPA treatment I/R gerbils markedly increased cell survival with palely stained nuclei compared with I/R group (0.71 ± 0.10 vs 0.60 ± 0.10, P < 0.01). NeuN immunohistochemistry was also employed to evaluated neuronal loss after global cerebral I/R. The results were consistent with Nissl staining (Fig. 2B and C) and the cell survival rates of VPA treatment I/R gerbils markedly increased compared with I/R group (0.73 ± 0.09 vs 0.54 ± 0.09, P < 0.01). Meanwhile, TUNEL immunofluorescence staining was detected to evaluated hippocampal neurons death. Our results indicated that VPA treatment I/R gerbils markedly decreased cell death with green stained nuclei compared with I/R group.

3.3. VPA protected hippocampal neuron against hypoxia/reoxygenation condition

To detect the anti-pyroptosis of VPA against hypoxia/reoxygenation condition in hippocampal neurons, the best concentrations of VPA were explored using MTT assay. As shown in Fig. 3A, hippocampal neurons treated with VPA (0.1–0.6 mM) revealed no obvious change in the levels of cell viability. 0.8 mM of VPA caused about 20% hippocampal neurons death. Especially, when hippocampal neurons suffer from hypoxia/reoxygenation condition, 0.6 mM of VPA has the greatest effect (Fig. 3B). Therefore, the addition of 0.6 mM VPA was used in the subsequent experiments. Hoechst 33342 staining result show 0.6 mM VPA can significantly increase hippocampal neurons survival rate compared with H/R group. The result of Hoechst 33342 staining

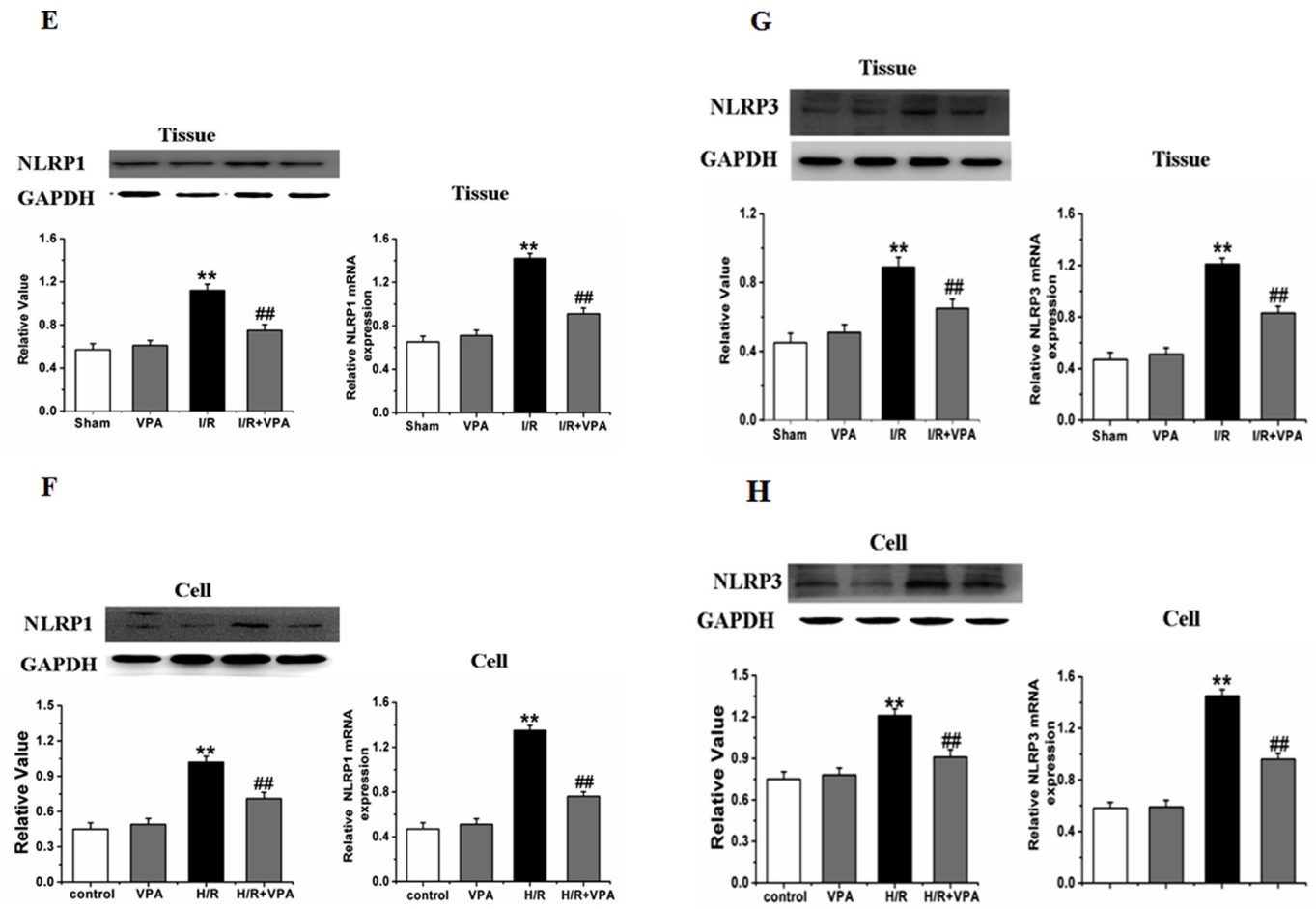

Fig. 5. (*continued*)

showed that the apoptosis rate of I/R + VPA group was reduced compared with I/R group (0.73 ± 0.09 vs 0.43 ± 0.07, P < 0.01) (Fig. 3C).

3.4. VPA regulates pro-pyroptosis factors IL-1β and IL-18

To exploit the potential role of VPA on neurons pyroptosis, we evaluated the effects of VPA on the expression of pro-pyroptosis factors IL-1β and IL-18 using enzyme-linked immunosorbent assay (ELISA) method. VPA significantly decreased IL-1β and IL-18 levels in ischemia/reperfusion hippocampus, which were similar after treatment with VPA in hypoxia/reoxygenation hippocampal neurons (Fig. 4A -B). The result was consistent with IL-1β and IL-18 mRNA change (Fig. 4C and D). We further evaluated the protein expression of IL-1β and IL-18 by western blot. The results demonstrated VPA significantly inhibited IL-1β and IL-18 levels in in vivo and in vitro (Fig. 4E and F). However, there is no effect on pro-IL-1β and pro-IL-18 expression.

3.5. VPA regulates the activity of caspase-1 and NLRP1 and NLRP3 inflammasome proteins

Caspase-1 and its active form gasdermin D can promote the activation of IL-1β and IL-18 and directly or through some signaling cascade leads to pyroptosis. Our results showed that ischemia/reperfusion increased caspase-1 and gasdermin D protein and gene level, and treatment with VPA, drastically decreased caspase-1 and gasdermin D compared with the control (Fig. 5A–D). Moreover, caspase-1 and gasdermin D level were elevated in hippocampal neurons seating in a hypoxia/reoxygenation environment, and this elevation was abolished by VPA, indicating that VPA attenuated caspase-1 and gasdermin D expression (Fig. 5A–D). As we know, caspase-1can be cleaved by NLRP1 and NLRP3. Therefore, the expression levels of the NLRP1 and NLRP3 was further investigated. Our results indicated that ischemia/reperfusion increased NLRP1 and NLRP3 protein and gene level, and treatment with VPA, drastically decreased NLRP1 and NLRP3 compared with the control in vivo and in vitro (Fig. 5E–H).

3.6. VPA regulates hippocampus pyroptosis through ARC

To examine whether ARC (an antiapoptotic gene) was implicated in ischemia/reperfusion or hypoxia/reoxygenation induced brain injury in hippocampal neurons. Firstly, the expression of ARC was investigated in the hippocampal neurons of brain. We found that ischemia/reperfusion decreased ARC at protein and gene level compared to the control group, which was significantly increased by treatment with VPA (Fig. 6A). A similar result in ARC change by treatment with VPA was observed in hypoxia/reoxygenation condition in hippocampal neurons (Fig. 6B).

Next, we transfected ARC siRNA into hippocampal neurons cell under hypoxia/reoxygenation conditions to confirm VPA protective effects through ARC signaling pathway. Firstly, we detected the transfection efficiency of siRNA mixtures by Fluorescent probe. The result showed that the transfection efficiency of siRNA mixtures is above 90% (Fig. 7A). Then, the ARC expression was detected by western blot. We found ARC expression was significantly decreased by siRNA mixtures (Fig. 7B). These results the ARC protein was successfully silenced. We observed a pronounced reduction of caspase-1, IL-1β, IL-18, NLRP1 and NLRP3 expression in VPA group compared with H/R group, but these effects can be reversed by silence of ARC (Fig. 7C–G). These results indicated that VPA inhibited pyroptosis though ARC pathway.

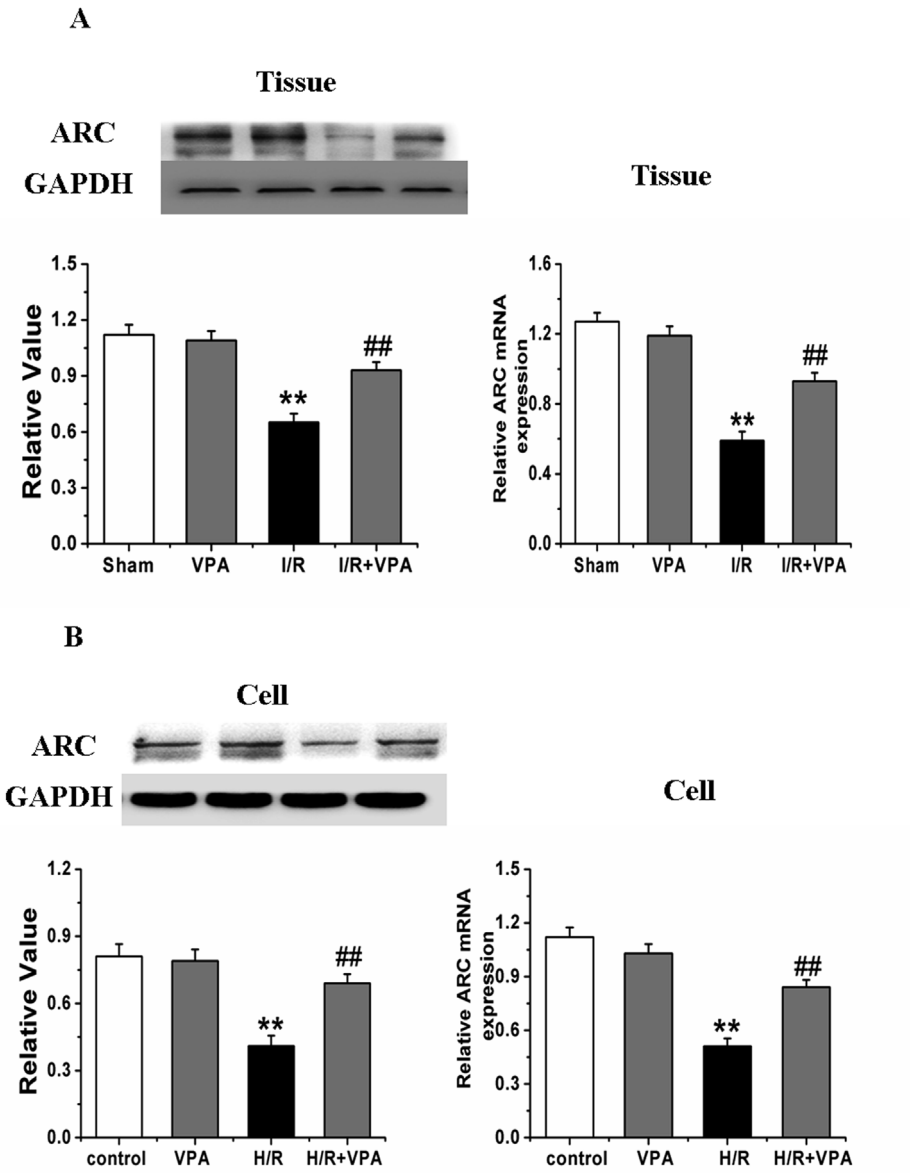

Fig. 6. VPA regulates the expression of ARC in vivo and in vitro. ARC protein and mRNA expression was detected in the gerbils hippocampal tissue (A) and hippocampal neurons (B). All the values are presented as mean ± SEM (n = 6 per group). **P < 0.01 compared to control group; ##P < 0.01 compared to H/R or I/R group.

4. Discussion

Cerebral ischemia/reperfusion injury is accompanied by a variety of cellular and molecular changes, which will increase permeability of capillaries and arterioles that lead to an increase of diffusion and fluid filtration across the tissues, finally resulted in stroke and brain trauma (Schaller and Graf, 2004). The underlying molecular mechanism was not clear. Here, to our knowledge, we first demonstrated that the potential effect of Valproic acid on cerebral molecular/cellular events during ischemia/reperfusion injury through ARC/caspase-1/IL-18, IL-1β pathway.

In the present study, we evaluated a novel role of VPA in a rat model of cerebral ischemia/reperfusion injury. VPA treatment significantly reversed learning and memory deficits in model gerbils by decreasing escape latency and the increasing number of times of platform passing. At same time, VPA treatment significantly reduced the neuronal death in vivo and in vitro. Furthermore, caspase-1 the key pyroptosis regulatory proteins, were also found to be remarkably changed in the VPA-treated ischemic gerbils. Collectively, these results suggested that VPA's neuroprotection against cerebral ischemia/reperfusion injury might be modulated through ARC/caspase-1/IL-18, IL-1β pathway.

Cerebral ischemia/reperfusion injury may occur in a variety of clinical settings including head trauma, postsurgical brain swelling, subarachnoid hemorrhage, stroke, and cardiac arrest (Schaller and Graf, 2004). In clinical, an increasing number of strategies have been developed for limiting or preventing further brain damage during reperfusion (Bruggen et al., 1999; Li et al., 2001; Rimpilainen et al., 2002; Wang et al., 2002). However, many promising strategies into effective therapies in humans have been disappointing. It is well known VPA would inhibit the activity of histone deacetylase (HDAC) directly and cause hyperacetylation of histones (Gottlicher, 2004). At same time, accumulated evidence demonstrated that HDAC inhibitors would alleviated the frequency of inflammation in some diseases, such as asthma and allergic diseases (Bhavsar et al., 2008; Blanchard and Chipoy, 2005). Peng et al. demonstrated that VPA prevents dopaminergic neurons from lipopolysaccharide-induced neurotoxicity through reducing

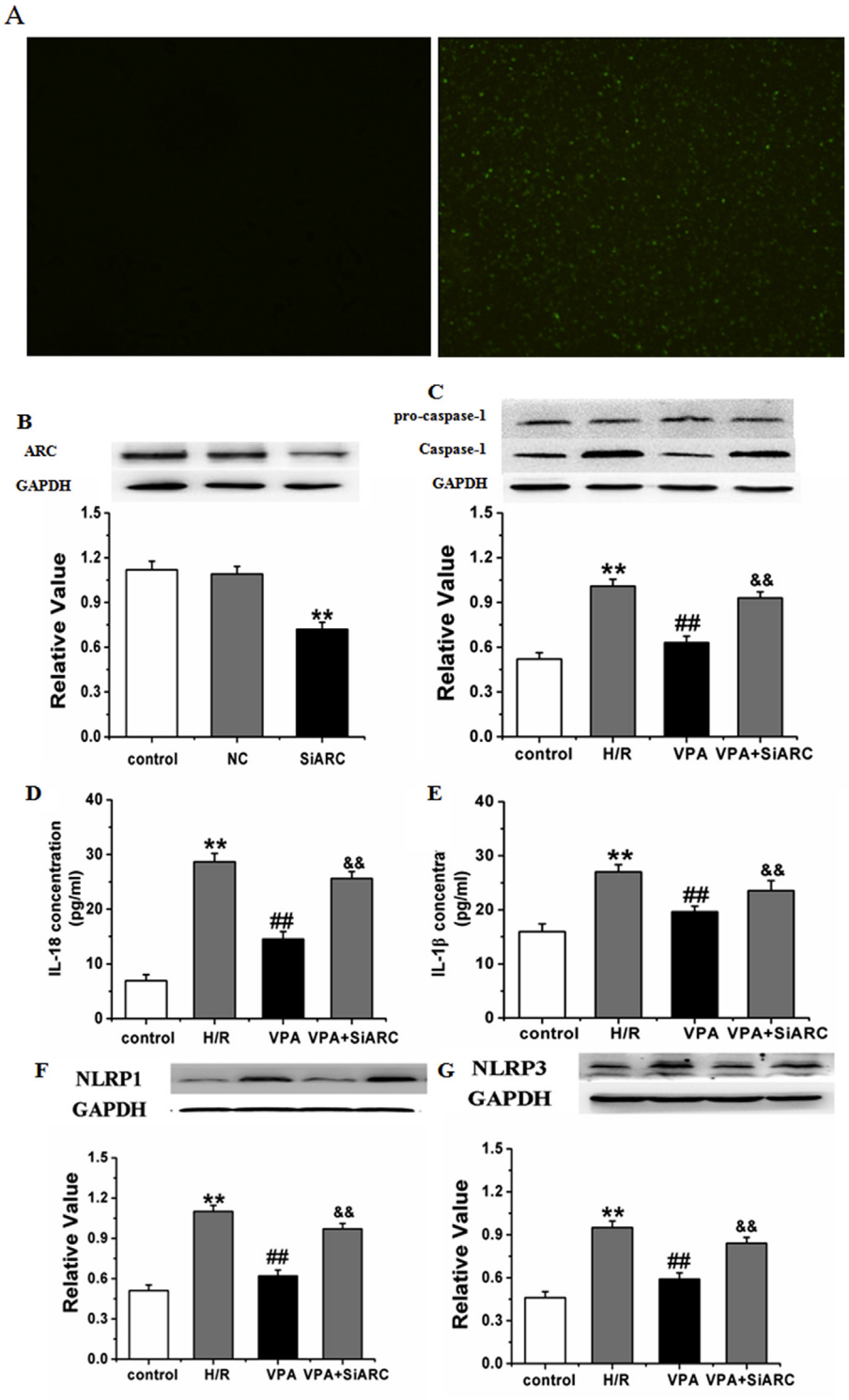

Fig. 7. Silence ARC pathway partially repeal the anti-pyroptosis effects of VPA. ARC was silenced successfully (A, B). ischemia/reperfusion injure increase hippocampal neurons caspase-1 activity (C), IL-1β and IL-18 concentrations in serum (D, E) and NLRP1(F) and NLRP3(G) expression compare with control group. These effects can be reversed by VPA. However, when silence ARC pathway, VPA anti-pyroptosis effects can be partially repeal. The data are expressed as the mean ± SEM (n = 6 per group). **P < 0.01 compared to control group; ##P < 0.01 compared to ischemia/reperfusion group.

the released of pro-inflammatory factors, which would be contributed to reduction of microglial cell number (Peng et al., 2005). Moreover, a recent study showed that VPA significantly inhibited MCAO-induced elevation of matrix metalloproteinase-9 and nuclear translocation of nuclear factor-κB (Wang et al., 2011). However, it is not known whether the VPA has protective effects on global cerebra ischemia/reperfusion injury is associated with inhibition of inflammatory. In our present study, we found that treatment with VPA significantly reversed learning and memory deficits in ischemia/reperfusion injury model. At same time, Nissl staining, NeuN immunohistochemistry showed that VPA treatment significantly reduced the neuronal injury in vivo. Furthermore, 0.6 mM of VPA significantly improves cell viability and

survival rate in oxygen-glucose deprivation hippocampal neuronal in vitro. These findings indicated that VPA alleviated ischemia/reperfusion injury in gerbils.

In subsequent experiments, we explore the mechanism of VPA on inhibition of ischemia/reperfusion injury. Pyroptosis is a highly inflammatory form of programmed cell death characterized by caspase-1 activation. In recent years, a tremendous amount of efforts have been devoted to exploring the mechanisms of pyroptosis in many diseases. Tan MS et al. reported that inhibition of pyroptosis was effective in either slowing or reducing cell injury in models of Alzheimer's disease (Tan et al., 2014). Our results showed that ischemia/reperfusion injury gerbils and hippocampal neurons cell which treat with oxygen-glucose deprivation displayed increased levels of caspase-1, IL-1β and IL-18. However, VPA could significantly decrease levels of caspase-1, IL-1β and IL-18 in the ischemia/reperfusion animal model and hippocampal neurons cell treated with oxygen-glucose deprivation to mimic ischemia/reperfusion. As we know, NLRP1 and NLRP3 can convert precursor caspase-1 into cleaved caspase-1 via proximity-induced autoactivation (Martinon et al., 2002). Activated NLRP3 together with the adaptor ASC protein forms a activating complex that activates Caspase-1. As we know, Caspase-1, highly expressed in the immune organs, would cleaves Gasdermin D into its active form, which leads to pyroptosis. Activated Caspase 1 also cleaves pro IL-1β into active forms, IL-1β. IL-1β is an important mediator of the inflammatory response, and promoted pyroptosis by a positive feedback mechanism that amplifies the inflammatory response. Therefore, we also examined the effect of VPA on NLRP1 and NLRP3. Our result indicated that VPA could also significantly decreased levels of NLRP1 and NLRP3 in the ischemia/reperfusion animal model and hippocampal neurons cell treated with oxygen-glucose deprivation. These results indicated that VPA protected neuronal cell injury by reduction of pyroptosis.

Apoptosis repressor with caspase recruitment domain (ARC), an antiapoptotic protein, is present in normal heart (Li et al., 2007, 2009) skeletal muscles (Koseki et al., 1998), and brain tissues (Hong et al., 2003) and protects them from apoptosis. Michael Neuss et al. demonstrated that ARC prevents oxidant stress-mediated cell death by preserving mitochondrial function (Neuss et al., 2001). Another study showed that ARC repressed cardiomyocyte pyroptosis in diabetic cardiomyopathy rats (Li et al., 2014). Our result showed that VPA increased the expression of ARC in vivo and in vitro. Further, we silenced ARC in hippocampal neuronal, the expression of NLRP1, NLRP3, caspase-1, IL-1β and IL-18 was increased in spite of treatment with VPA. These results indicated that VPA protected neuronal cell pyroptosis by regulation ARC protein.

5. Conclusion

The present study identified VPA as a crucial regulator of cerebral ischemia/reperfusion injury. The protective effects of VPA may be resistance to neuronal cell pyroptosis through ARC/NLRP1/NLRP3/caspase-1/IL-1β/IL-18 pathway. Since VPA is a well-established drug for a long term clinical therapy, it might be promising as a candidate therapy for human ischemia stroke.

Acknowledgments

This study was supported by grants from National Natural Science Foundation of China, (81202834), Liaoning Provincial Science Fund Guidance Program (20180551110), the open fund of the key Laboratory of Ministry of Education for Traditional Chinese Medicine Viscera-State Theory and Applications of Liaoning University of Traditional Chinese Medicine (zyzx1705) and the Youth Project Funds from Department of Education of Liaoning Province (L201716).

Appendix A. Supplementary data

Supplementary data to this article can be found online at https://doi.org/10.1016/j.neuint.2019.01.003.

References

Almeida, R.D., Manadas, B.J., Melo, C.V., Gomes, J.R., Mendes, C.S., Graos, M.M., et al., 2005. Neuroprotection by BDNF against glutamate-induced apoptotic cell death is mediated by ERK and PI3-kinase pathways. Cell Death Differ. 12, 1329–1343.
Bhavsar, P., Ahmad, T., Adcock, I.M., 2008. The role of histone deacetylases in asthma and allergic diseases. J. Allergy Clin. Immunol. 121, 580–584.
Blaheta, R.A., Michaelis, M., Driever, P.H., Cinatl Jr., J., 2005. Evolving anticancer drug valproic acid: insights into the mechanism and clinical studies. Med. Res. Rev. 25, 383–397.
Blanchard, F., Chipoy, C., 2005. Histone deacetylase inhibitors:new drugs for the treatment of inflammatory diseases? Drug Discov. Today 10, 197–204.
van Bruggen, N., Thibodeaux, H., Palmer, J.T., et al., 1999. VEGF antagonism reduces edema formation and tissue damage after ischemia/reperfusion injury in the mouse brain. J. Clin. Invest. 104, 1613–1620.
Byrne, B.G., Dubuisson, J.F., Joshi, A.D., Persson, J.J., Swanson, M.S., 2013. Inflammasome components coordinate autophagy and pyroptosis as macrophage responses to infection. mBio 4 e00620-12.
Coll, N.S., Epple, P., Dangl, J.L., 2011. Programmed cell death in the plant immune system. Cell Death Differ. 18, 1247–1256.
Donnan, G.A., Fisher, M., Macleod, M., Davis, S.M., 2008. Stroke. Lancet 371, 1612–1613.
Fantuzzi, G., Dinarello, C.A., 1999. Interleukin-18 and interleukin-1 beta: two cytokine substrates for ICE (caspase-1). J. Clin. Immunol. 19, 1–11.
Goldstein, L.B., Rothwell, P.M., 2008. Advances in prevention and health services delivery. Stroke 39, 258–260.
Gottlicher, M., 2004. Valproicacid:an old drug newly discovered as inhibitor of histone deacetylase. Ann. Hematol. 83, S91–S92.
Gurvich, N., Klein, P.S., 2002. Lithium and valproic acid:Parallels and contrasts in diverse signaling contexts. Pharmacol. Ther. 96, 45–66.
Hong, Y.M., Jo, D.G., Lee, J.Y., et al., 2003. Down-regulation of ARC contributes to vulnerability of hippocampal neurons to ischemia/hypoxia. FEBS Lett. 543, 170–173.
Kim, H.J., Rowe, M., Ren, M., Hong, J.S., Chen, P.S., Chuang, D.M., 2007. Histone deacetylase inhibitors exhibit antiinflammatory and neuroprotective effects in a rat permanent ischemic model of stroke: multiple mechanisms of action. J. Pharmacol. Exp. Therapeut. 321, 892–901.
Koseki, T., Inohara, N., Chen, S., Nunez, G., 1998. ARC, an inhibitor of apoptosis expressed in skeletal muscle and heart that interacts selectively with caspases. Proc. Natl. Acad. Sci. Unit. States Am. 95, 5156–5160.
Kroemer, G., Galluzzi, L., Vandenabeele, P., Abrams, J., Alnemri, E.S., Baehrecke, E.H., 2009. Classification of cell death: recommendations of the nomenclature committee on cell death. Cell Death Differ. 16, 3–11.
Li, P.A., He, Q.P., Nakamura, L., et al., 2001. Free radical spin trap alpha-phenyl-N-tert-butylnitron inhibits caspase-3 activation and reduces brain damage following a severe forebrain ischemic injury. Free Radic. Biol. Med. 31, 1191–1197.
Li, X., Du, N., Zhang, Q., Li, J., et al., 2014. MicroRNA-30d regulates cardiomyocyte pyroptosis by directly targeting foxo3a in diabetic cardiomyopathy. Cell Death Dis. 5, e1479.
Li, Y., Ge, X., Liu, X., 2009. The cardioprotective effect of postconditioning is mediated by ARC through inhibiting mitochondrial apoptotic pathway. Apoptosis 14, 164–172.
Li, Y.Z., Liu, X.H., Zhu, X.M., Cai, L.R., 2007. ARC contributes to the inhibitory effect of preconditioning on cardiomyocyte apoptosis. Apoptosis 12, 1589–1595.
Martinon, F., Burns, K., Tschopp, J., 2002. The inflammasome: a molecular platform triggering activation of inflammatory caspases and processing of proIL-beta. Mol. Cell 10, 417–426.
Neuss, M., Monticone, R., Lundberg, M.S., Chesley, A.T., Fleck, E., Crow, M.T., 2001. The apoptotic regulatory protein ARC (apoptosis repressor with caspase recruitment domain) prevents oxidantstress-mediated cell death by preserving mitochondrial function. J. Biol. Chem. 276, 33915–33922.
Peng, G.S., Li, G., Tzen, N.S., Chen, P.S., Chuang, D.M., Hsu, Y.D., Yang, S., Hong, J.S., 2005. Valproate pretreatment protects dopaminergic neurons from LPS induced neurotoxicity in rat primary midbrain cultures: role of microglia. Brain Res Mol Brain Res 134, 162–169.
Rimpilainen, J., Romsi, P., Pokela, M., et al., 2002. Lamotrigine plus leukocyte filtration as a neuroprotective strategy in experimental hypothermic circulatory arrest. Ann. Thorac. Surg. 73, 163–172.
Schaller, B., Graf, R., 2004. Cerebral ischemia and reperfusion: the pathophysiologic concept as a basis for clinical therapy. J. Cerebr. Blood Flow Metabol. 24, 351–371.
Tan, M.S., Tan, L., Jiang, T., Zhu, X.C., Wang, H.F., Jia, C.D., Yu, J.T., 2014. Amyloid-β induces NLRP1-dependent neuronal pyroptosis in models of Alzheimer's disease. Cell Death Dis. 21 (5) e1382.
Wang, G.J., Deng, H.Y., Maier, C.M., et al., 2002. Mild hypothermia reduces ICAM-1 expression, neutrophil infiltration and microglia/monocyte accumulation following experimental stroke. Neuroscience 114, 1081–1090.
Wang, Z., Leng, Y., Tsai, L.K., Leeds, P., Chuang, D.M., 2011. Valproic acid attenuates blood-brain barrier disruption in a ra tmodel of transient focal cerebral ischemia: the roles of HDAC and MMP-9 inhibition. J. Cerebr. Blood Flow Metabol. 31, 52–57.
Wu, Y., Ding, A.S., Wu, L.Y., Ma, Z.M., Fan, M., 2003. Establishment of the model of oxygen-glucose deprivation in vitro rat hippocampal neurons. Chin. J. Appl. Physiol. 19, 197–200.
Xu, J., Jiang, Y., Wang, J., Shi, X., et al., 2014. Macrophage endocytosis of high-mobility group box 1 triggers pyroptosis. Cell Death Differ. 21, 1229–1239.
Zhang, Y.B., Kan, M.Y., Yang, Z.H., Ding, W.L., Yi, J., Chen, H.Z., Lu, Y., 2009. Neuroprotective effects of N-stearoyltyrosine on transient global cerebral ischemia in gerbils. Brain Res. 1287, 146–156.
Zhang, Z., Zhang, Z.Y., Wu, Y., Schluesener, H.J., 2012. Valproic acid ameliorates inflammation in experimental autoimmune encephalomyelitis rats. Neuroscience 221, 140–150.